New Journal of Physics
The open-access journal for physics

Asymptotic dynamics of qubit networks under randomly applied controlled unitary transformations

J Novotný[1,2,3], G Alber[2] and I Jex[1]

[1] Department of Physics, FNSPE, Czech Technical University in Prague, Břehová 7, 115 19 Praha 1, Staré Město, Czech Republic
[2] Institut für Angewandte Physik, Technische Universität Darmstadt, D-64289 Darmstadt, Germany
E-mail: novotny.jaroslav@seznam.cz

New Journal of Physics **13** (2011) 053052 (27pp)
Received 3 December 2010
Published 26 May 2011
Online at http://www.njp.org/
doi:10.1088/1367-2630/13/5/053052

Abstract. The asymptotic dynamics of many-qubit quantum systems is investigated under iteratively and randomly applied unitary transformations. For a one-parameter family of unitary transformations, which entangle pairs of qubits, two main theorems are proved. They characterize completely the dependence of the resulting asymptotic dynamics on the topology of the interaction graph that encodes all possible qubit couplings. These theorems exhibit clearly which aspects of an interaction graph are relevant and which ones are irrelevant to the asymptotic dynamics. On the basis of these theorems, the local entropy transport between an open quantum system and its environment are explored for strong non-Markovian couplings and for different sizes of the environment and different interaction topologies. It is shown that although the randomly applied unitary entanglement operations cannot decrease the overall entropy of such a qubit network, a local entropy decrease or 'cooling' of subsystems is possible for special classes of interaction topologies.

[3] Author to whom any correspondence should be addressed.

Contents

1. Introduction

The development of sophisticated experimental cooling and trapping techniques has enabled the controlled manipulation of many-qubit quantum systems to an unprecedented level of sophistication. Thus, in the spirit of Feynman's original suggestion [1], it has become possible to simulate interesting Hamiltonian dynamics with the help of elementary qubit systems whose interactions are engineered appropriately by external laser fields, for example [2]. These quantum technological developments also allow us to explore new dynamical regimes of open non-Hamiltonian many-qubit dynamics in which couplings between different qubits are caused not by direct Hamiltonian interactions but by additional ancilla systems and by projective measurements [3]. Such open many-qubit systems may be viewed as quantum generalizations of classical bit networks that already play a central role in various branches of classical physics and that have been explored extensively in recent decades [4]. Quantum networks are also of topical interest in quantum information science in the form of quantum communication or quantum computation networks [5]. Typical nodes of these types of networks are material quantum systems, which are entangled by photonic quantum channels, for example. In the simplest possible cases, the nodes of such a network are qubit systems. Recently, numerous theoretical proposals have been developed on how such types of quantum networks can be implemented by present-day technology, and first promising experimental results are already available [5, 6]. Thus, quantum networks, i.e. qubit systems that are coupled and entangled by quantum operations [7], constitute a unifying concept with which numerous fundamental characteristic quantum phenomena can be explored all the way from the microscopic to the macroscopic domain. In particular, their dynamical features and their scaling properties shed new light on basic questions concerning entanglement and decoherence [8, 9].

Incomplete control over couplings between the nodes of a quantum network introduces randomness, which typically affects characteristic quantum phenomena, such as quantum interference and entanglement. It has been demonstrated recently that in large quantum systems, this randomness may offer interesting, and at first sight apparently counter-intuitive, possibilities

for enabling or enhancing physical processes of practical interest, such as energy transfer in light-harvesting complexes [10] or transmission of quantum information in qubit networks [11]. Motivated by these recent developments, in this paper, we address the question of how classical randomness influences the entanglement properties of quantum networks. For this purpose, we investigate the asymptotic dynamics of arbitrarily sized qubit networks under the influence of repeatedly and randomly applied unitary two-qubit entanglement operations. In the context of quantum communication networks, for example, such a classical randomness may result from the uncontrolled influence of users who entangle different pairs of nodes of the network in a random way. In the different context of quantum information processors, this randomness may arise from shift register, for example, which entangles arrays of trapped atomic qubits in an uncontrolled way [12]. In the framework of 'collision models' [13–17], for example, this randomness describes the lack of knowledge about subsequent 'collisions' that entangle pairs of distinguishable interacting particles. The unitary entanglement operations considered here are assumed to belong to a particular one-parameter family of two-qubit transformations, which also contains the controlled-NOT operation as a special case. It is shown that for this type of entanglement operations, the resulting asymptotic dynamics of the qubit network can be determined analytically. Thus, within this exactly solvable model, interesting general relations can be established between asymptotic quantum states and their corresponding interaction topology, i.e. the system of all two-qubit entanglement operations that are possible within such a qubit network. These relations exhibit in a quantitative way the intricate interplay between entanglement and classical noise and the resulting balance that characterizes the asymptotic quantum states. Furthermore, it is demonstrated that although classical randomness is involved in the network, the entropy of subsystems may decrease. As our results are valid for arbitrarily sized qubit networks, interesting conclusions concerning scaling properties can also be drawn. In particular, for moderate numbers of qubits, the effects predicted should be amenable to further experimental exploration.

In the following, two main theorems are derived that characterize the asymptotic dynamics of arbitrarily sized qubit networks whose couplings are determined by the already mentioned one-parameter family of randomly applied controlled unitary transformations. These results emphasize the significance of the interaction topology of the network, i.e. of the structure of the possible two-qubit couplings that take place with non-zero probabilities. Furthermore, they demonstrate clearly which details of this topology are relevant for determining the asymptotic dynamics of such qubit networks and which ones are irrelevant. These general results are applied to exploring a characteristic many-qubit phenomenon in detail, namely the local entropy exchange between an open subsystem of such a randomly interacting qubit network and its residual qubit environment. Contrary to previous investigations of open quantum systems [13–18], on the basis of our two main theorems, this phenomenon can be explored without any further simplifying assumptions concerning the number of relevant couplings between the system and environment qubits, concerning their initial state or the numbers of qubits involved. In this way, interesting aspects concerning the dependence of the asymptotic dynamics on the size of the qubit network and on the topology of the relevant interaction graph can be explored in detail for strong couplings in the non-Markovian domain. Furthermore, it should be mentioned that in our subsequent treatment, no constraints are imposed on the form of the possible initial states of the system and environment.

This paper is organized as follows. Starting from our recently developed general theoretical framework [19, 20], in section 2 we summarize relevant previously derived results concerning

the asymptotic dynamics of quantum systems under the influence of iteratively applied random unitary transformations. In particular, we discuss important consequences of these results for the qubit networks being investigated here. In addition, the concept of an interaction graph is introduced that encodes in a convenient way the topological properties of a randomly interacting qubit network by characterizing which qubits interact with non-zero probabilities. In section 3, the asymptotic dynamics of a special one-parameter family of conditional unitary two-qubit transformations is investigated, which contains the controlled-NOT operation as a special case. Two main results are proved in the form of theorems. Firstly, it is shown that all qubit networks with strongly connected interaction graphs share the same asymptotic dynamics. Secondly, a generalization of this theorem is presented that also characterizes the asymptotic dynamics of qubit networks with non-strongly connected interaction graphs. For the one-parameter family of controlled unitary couplings considered in this paper, these two main results show clearly which aspects of a randomly coupled qubit network are relevant and which ones are irrelevant to its asymptotic dynamics. In section 4, details of the resulting local entropy exchange between an open system and its environment are investigated analytically. We show that, in spite of a non-decreasing entropy of the composite system, the non-Markovian evolution of the local subsystem allows us to drain some of its entropy into the environment. With the help of two main theorems derived previously by us, we study the entropy flow in two basic settings. In the first setting, the composite system forms a strongly connected qubit network. It is shown that in this case, both thermalization and cooling, i.e. maximization and reduction of the entropy of the open subsystem, can be achieved. In the second setting, we assume that only the open system forms a strongly connected qubit network and all environmental qubits act as target qubits as far as the coupling between the open system and its environment is concerned. It is proved that in this case, neither thermalization nor cooling can be achieved. Moreover, it is shown that the asymptotic dynamics of the open system is independent of the way the environmental qubits are coupled among themselves. Thus, in the asymptotic regime, the open system does not undergo any changes in the couplings of the environmental qubits, so that this part of the qubit network is irrelevant as far as the asymptotic dynamics of the open subsystem are concerned.

2. Asymptotic dynamics of randomly interacting qubit networks

Let us consider a typical quantum network, i.e. an open quantum system consisting of N qubits interacting with each other by the repeated application of a single unitary two-qubit interaction $\hat{U}$, which is applied to pairs of qubits according to a prescribed probability distribution. Information as to which qubit pairs are coupled with which probabilities within this quantum network can be encoded in a convenient way by a weighted and directed interaction graph (or digraph) $\mathsf{G}(\mathsf{E}, \mathsf{V})$. Its N vertexes $i \in \mathsf{V} = \{1, \ldots, N\}$ represent the N qubits and its $m \leqslant N(N-1)/2$ directed edges $e = ij \in \mathsf{E} = \{i_1 j_1, \ldots, i_m j_m\}$ with weights p_{ij} encode the probabilities $p_{ij} > 0$ with which qubits i and j are coupled by the unitary two-qubit transformation $\hat{U}_{ij}$. These probabilities are normalized according to $\sum_{e \in \mathsf{E}} p_e = 1$. As a qubit of such a quantum network does not interact with itself, the corresponding interaction graph $\mathsf{G}(\mathsf{E}, \mathsf{V})$ contains neither loops nor multiple edges (compare with figure 1). If the coupling $\hat{U}_{ij}$ involves qubits i and j in an asymmetric way, as in the case of a controlled-NOT operation, for example, this is indicated by an arrow whose head is j and whose tail is i.

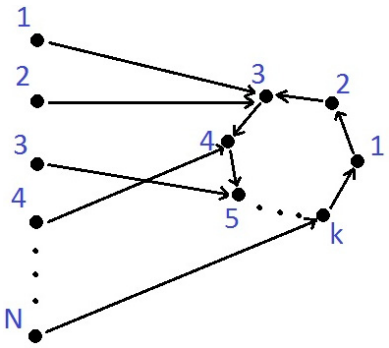

Figure 1. Example of a (non-strongly connected) interaction graph: vertexes connected by a directed edge represent qubits that interact with non-zero probabilities by a unitary conditional two-qubit transformation. In a controlled unitary transformation, the target qubit is the head and the control qubit is the tail of the directed edge.

After a single application of a random unitary two-qubit interaction $\hat{U}$, an originally prepared quantum state $\hat{\rho}(n)$ of such an N-qubit network is changed according to

$$\hat{\rho}(n) \longrightarrow \hat{\rho}(n+1) = \sum_{e \in \mathsf{E}} p_e \hat{U}_e \hat{\rho}(n) \hat{U}_e^\dagger := \mathcal{P}_{\mathsf{G}}(\hat{\rho}(n)), \tag{1}$$

with $\hat{U}_e$ denoting the two-qubit interaction acting on qubits i and j, which constitute the edge $e := ij$ of the interaction graph $\mathsf{G}(\mathsf{E}, \mathsf{V})$. The state change (1) is generated by the linear superoperator $\mathcal{P}_{\mathsf{G}}$, which is characterized by the interaction graph $\mathsf{G}(\mathsf{E}, \mathsf{V})$ and which cannot be diagonalized in general. It acts on the Hilbert space $\mathcal{B}(\mathscr{H})$ of linear operators over the Hilbert space $\mathscr{H} \equiv \mathbb{C}^{2N}$ of N qubits. In general, a quantum operation of the form (1) with Kraus operators $\{\hat{K}_e := \sqrt{p_e}\hat{U}_e, e \in \mathsf{E}\}$ is called a random unitary operation [21] and it belongs to the class of trace-preserving unital quantum channels [22]. In our subsequent discussion, we want to explore the asymptotic quantum states $\hat{\rho}(n)$ resulting from an initially prepared quantum state $\hat{\rho}_{\mathrm{in}}$ in the limit of large numbers of iterations n.

The general properties of the asymptotic longtime dynamics resulting from random unitary operations (1) have been studied recently for general cases that do not necessarily involve qubit systems [19, 20]. So, let us briefly recapitulate some of these results and discuss their consequences for the special kind of random unitary dynamics that we are investigating in this work.

It has been shown that the asymptotic iterative longtime dynamics of a random unitary trace-preserving map $\mathcal{P}$ which acts on density operators $\hat{\rho}_{\mathrm{in}} \in \mathcal{B}(\mathscr{H})$ are determined by an asymptotic attractor space $\mathsf{Atr}(\mathcal{P})$. For a given interaction graph $\mathsf{G}(\mathsf{V}, \mathsf{E})$, this attractor space is constructed by all linearly independent solutions $\hat{X}_{\lambda,i} \in \mathcal{B}(\mathscr{H})$ of the eigenvalue equations

$$\hat{U}_e \hat{X}_{\lambda,i} \hat{U}_e^\dagger = \lambda \hat{X}_{\lambda,i} \quad \text{for all } e \in \mathsf{E}. \tag{2}$$

In particular, it has also been shown that this attractor space is the direct sum of all eigenspaces of this set of equations belonging to different eigenvalues λ with $|\lambda| = 1$. These eigenvalues constitute the attractor spectrum $\sigma_{|1|}$. This is due to the fact that the Hilbert space $\mathcal{B}(\mathscr{H})$ can be decomposed into a direct sum according to $\mathcal{B}(\mathscr{H}) = \mathsf{Atr}(\mathcal{P}) \oplus (\mathsf{Atr}(\mathcal{P}))^\perp$ with $\perp$ denoting

the orthogonal complement, and that both mutually orthogonal subspaces are invariant under iterations of random unitary operations. Furthermore, all components in the subspace $(\mathsf{Atr}(\mathcal{P}))^{\perp}$ vanish after sufficiently large numbers of iterations. Thus, in the asymptotic limit of large numbers of iterations n, the dynamics are described by the relation

$$\hat{\rho}(n) = \mathcal{P}^n(\hat{\rho}_{\mathrm{in}}) = \sum_{|\lambda|=1, i=1}^{D_\lambda} \lambda^n \mathrm{Tr}\{\hat{\rho}_{\mathrm{in}} \hat{X}^{\dagger}_{\lambda,i}\} \hat{X}_{\lambda,i}, \tag{3}$$

with D_λ denoting the dimension of the eigenspace defined by (2) corresponding to the eigenvalue λ. In (3), it is assumed that the linear independent solutions $\hat{X}_{\lambda,i}$ of (2) are orthogonal and normalized in the sense $\mathrm{Tr}\{\hat{X}^{\dagger}_{\lambda,i} \hat{X}_{\lambda',i'}\} = \delta_{\lambda\lambda'}\delta_{ii'}$.

These general results have interesting consequences for the randomly interacting qubit networks that we are investigating here:

- The set of attractors is independent of the values of the probabilities p_e with which two qubits i and j are coupled by the edge $e = ij$. Thus, all interaction graphs with the same numbers of qubits and the same set of edges E (associated with non-zero probabilities) have the same attractor space $\mathsf{Atr}(\mathcal{P}_{\mathsf{G}})$. The actual values of the non-zero probabilities determine only how fast an initially prepared state $\hat{\rho}_{\mathrm{in}}$ converges to the asymptotic dynamics.
- Let us consider two interaction graphs, say G and H, with the property that one of them is a subset of the other one, say $\mathsf{H} \subseteq \mathsf{G}$, but with the same number of qubits, i.e. vertexes. Thus, the set of attractors $\mathsf{Atr}(\mathcal{P}_{\mathsf{G}})$ of the interaction graph G is a subset of the set of attractors $\mathsf{Atr}(\mathcal{P}_{\mathsf{H}})$ of the interaction graph H, i.e.

$$\mathsf{H} \subseteq \mathsf{G} \Rightarrow \mathsf{Atr}(\mathcal{P}_{\mathsf{G}}) \subseteq \mathsf{Atr}(\mathcal{P}_{\mathsf{H}}). \tag{4}$$

  This is due to the fact that the attractors of G have to fulfill more constraints according to (2). Therefore, if the sets of attractors of the interaction graphs H and G are equal, an arbitrary interaction graph F with the property $\mathsf{H} \subseteq \mathsf{F} \subseteq \mathsf{G}$ has also the same set of attractors as G. A simple consequence of these relations is that there is always a minimal set of the so-called *base attractors*, which is included in the set of attractors of all possible interaction graphs with the same numbers of qubits. The base attractors are the elements of the attractor space of the complete interaction graph in which each qubit is coupled to each other one and vice versa with a non-zero probability (compare with figure 2(a)). These base attractors are determined uniquely by a particular unitary two-qubit interaction $\hat{U}$. Interaction graphs that have just this minimal set of attractors we call *base graphs*. Apparently, base graphs play an important role in the solution and classification of the asymptotic dynamics of general randomly interacting quantum networks because they exhibit clearly which couplings are relevant for achieving a particular attractor space and which ones are irrelevant.

3. Asymptotic dynamics of controlled unitary interactions

According to (2) and (3), the asymptotic quantum states of randomly interacting qubit networks depend not only on the specific form of the unitary interaction $\hat{U}$ but also on the topology of the interaction graph $\mathsf{G}(\mathsf{E}, \mathsf{V})$ involved, i.e. on the information as to which qubits are connected by which edges. Motivated by the significant role that controlled unitary transformations play in the processing of quantum information [5] and on a more fundamental level in our understanding

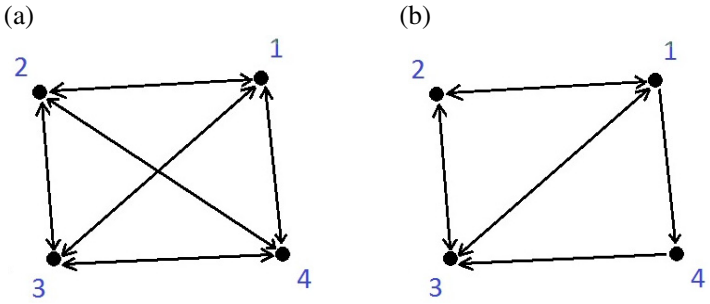

Figure 2. Interaction graphs representing qubit networks: completely (a) and strongly (b) connected interaction graphs in which any two qubits i and j are coupled in both directions with non-zero probabilities, either by a directed edge, in the case of complete connectedness, or at least by one path formed by adjacent directed edges, in the case of strong connectedness.

of decoherence and the emergence of classical features [8], we explore these dependences for a one-parameter family of conditional two-qubit couplings. This family of unitary transformations also includes the controlled-NOT transformation as a special case. For these couplings, two main results are shown. Firstly, it is proved that it is exactly the set of all strongly connected interaction graphs which for a given number of qubits yields the base attractors. Thus, full details of an interaction graph apart from its strong connectedness are irrelevant to the attractor space and therefore to the resulting asymptotic dynamics. Secondly, it is proved that the attractor spaces of non-strongly connected interaction graphs are determined uniquely by the corresponding digraph of continuity. Thus, also for this significantly more general class of interaction graphs, the aspects of the dynamical couplings between the qubits that are relevant to the asymptotic dynamics can be characterized completely.

Controlled unitary two-qubit interactions are asymmetric. One qubit constitutes the control and the other one the target. The asymmetry of the interaction originates from the fact that the quantum state of the target qubit is changed conditional on the quantum state of the control qubit and that there are at least two orthogonal quantum states of the control qubit, i.e. the so-called computational basis states, which are not affected by this interaction at all. In order to put the problem into perspective, let us consider a particular one-parameter family of controlled unitary two-qubit couplings acting on the control and target qubits i and j according to

$$\hat{U}_{ij}^{(\phi)} = |0\rangle_{ii}\langle 0| \otimes \hat{I}_j + |1\rangle_{ii}\langle 1| \otimes \hat{u}_j^{(\phi)} \tag{5}$$

with

$$\hat{u}_j^{(\phi)} = \cos\phi\,(|0\rangle_{jj}\langle 0| - |1\rangle_{jj}\langle 1|) + \sin\phi\,(|0\rangle_{jj}\langle 1| + |1\rangle_{jj}\langle 0|) \tag{6}$$

and with $\hat{I}_j$ denoting the unit operator acting on qubit j. For $\phi = 0$ or $\phi = \pi$, the two-qubit unitary transformation $\hat{U}^{(\phi)}$ is diagonal in the (orthonormal) computational basis $\{|00\rangle, |01\rangle, |10\rangle, |11\rangle\}$ and it describes a conditional phase change of magnitude π of one of the target states of qubit j. In the special case $\phi = \pi/2$, the controlled unitary transformation $\hat{U}_{ij}^{(\phi)}$ reduces to a controlled-NOT operation with control qubit i and target qubit j. The unitary transformation (6) is Hermitian and its eigenvalues λ are given by $\lambda_1 = 1$ and $\lambda_2 = -1$ with

corresponding eigenvectors $|V_1\rangle$ and $|V_1^{\perp}\rangle$. Hence, for an arbitrary interaction graph $\mathsf{G}(\mathsf{V},\mathsf{E})$, the superoperator of the associated random unitary transformation, i.e.

$$\Phi(.) = \sum_{e\in\mathsf{E}} p_e \hat{U}_e^{(\phi)}(.)\hat{U}_e^{\dagger(\phi)}, \tag{7}$$

is also Hermitian and its attractor spectrum $\sigma_{|1|}$ fulfills the relation $\sigma_{|1|} \subset \{-1, 1\}$.

Furthermore, in our subsequent discussion, we restrict ourselves to cases with $\phi \in (0, \pi)$. As already mentioned, if $\phi = 0$ or $\phi = \pi$, all controlled operations $\hat{U}_e^{(\phi)}$ are diagonal in the computational basis and therefore the superoperator (7) is also diagonal, so that a solution of the asymptotic dynamics is significantly simpler than for general parameters $\phi \in (0, \pi)$.

3.1. Base attractors and base graphs

As already stated in section 2, base attractors are the minimal building blocks of the attractor spaces of arbitrary interaction graphs because they are elements of the attractor space of any quantum network with the same number of qubits. For a given number of qubits N, these base attractors are determined uniquely by a given unitary two-qubit interaction $\hat{U}$ and by the completely connected interaction graph in which each of these N qubits is coupled to each other one and *vice versa* (see figure 2(a)).

In view of the important role of base attractors in the construction of attractor spaces of any interaction graph, it is of primary interest to determine the structure of the most general quantum networks whose associated attractor space consists of base attractors only. Let us call their interaction graphs base graphs. Definitely, the completely connected interaction graph is an example of a base graph but, depending on the two-qubit transformation $\hat{U}$ under consideration, typically it is not the only one. For the one-parameter family of conditional unitary two-qubit interactions (5) with $\phi \neq 0, \pi$ the base graphs are characterized completely by the following theorem:

Theorem 3.1. *For $\phi \neq 0, \pi$ the base graphs of the one-parameter family of conditional unitary two-qubit interactions (5) are exactly all strongly connected interaction graphs $\mathsf{G}(\mathsf{V},\mathsf{E})$ in which any pair of vertexes is connected by some path (i.e. a connected sequence of directed edges) in both directions. For a given number of qubits with $N \geqslant 3$, the associated base attractors are elements of a five-dimensional (5D) attractor space $\mathsf{Atr}(\Phi_{\mathsf{G}})$. An orthonormal basis system of linear operators in this space of base attractors is given by*

$$\begin{aligned} &\hat{X}_1 = |\mathbf{0}_N\rangle\langle\mathbf{0}_N|, \quad \hat{X}_2 = |\mathbf{0}_N\rangle\langle\psi_N|, \quad \hat{X}_3 = |\psi_N\rangle\langle\mathbf{0}_N|, \quad \hat{X}_4 = |\psi_N\rangle\langle\psi_N|, \\ &\hat{X}_5 = (\hat{I}_N - |\mathbf{0}_N\rangle\langle\mathbf{0}_N| - |\psi_N\rangle\langle\psi_N|)/\sqrt{2^N - 2} \end{aligned} \tag{8}$$

with the pure N-qubit states

$$\begin{aligned} |\mathbf{0}_N\rangle &= |0\rangle^{\otimes N}, \ |\psi_N\rangle = |\theta_N\rangle/\sqrt{\langle\theta_N|\theta_N\rangle}, \\ |\theta_N\rangle &= \sum_{0\neq z\in \mathsf{I}_N} \left(\cos\frac{\phi}{2}\right)^{N-\tau(z)} \left(\sin\frac{\phi}{2}\right)^{\tau(z)} |z\rangle. \end{aligned} \tag{9}$$

Thereby, I_N denotes the set of all possible binary N-tuples and $\tau(z)$ is the sum of the bit values of all N qubits of the N-qubit string z. All of these base attractors (8) solve equations (2) with eigenvalue $\lambda = 1$. For $N \geqslant 3$ there are no non-trivial solutions of (2) with eigenvalue $\lambda = -1$.

In the special case of two qubits, i.e. $N = 2$, the attractor space $\mathsf{Atr}(\Phi_{\mathsf{G}})$ of the base attractors is 6D. There is a 5D eigensubspace given by (2) associated with eigenvalue $\lambda = 1$ whose orthonormal basis is again given by (8). But now, also a non-trivial 1D eigensubspace exists that corresponds to eigenvalue $\lambda = -1$ and that contains the normalized linear operator,

$$\hat{X}_6 = (\cos(\phi/2)(|01\rangle\langle 11| - |10\rangle\langle 11| - |11\rangle\langle 01| + |11\rangle\langle 10|) - \sin(\phi/2)(|01\rangle\langle 10| - |10\rangle\langle 01|))/\sqrt{2+2\cos^2(\phi/2)}. \tag{10}$$

Although it is straightforward to prove that the linear operators (8) and (10) solve equations (2) with the corresponding eigenvalues, the proof that they also form a basis of the minimal attractor space is less apparent. Thus, a formal proof of theorem 3.1 based on graph theoretical methods is given in appendix.

For the generic case of $N \geqslant 3$, this theorem tells us that all attractors have eigenvalue $\lambda = 1$. Thus, asymptotically any initially prepared quantum state $\hat{\rho}_{\text{in}}$ approaches the stationary state,

$$\hat{\rho}_{\infty} = p\frac{\hat{P}_N\hat{\rho}_{\text{in}}\hat{P}_N}{p} + (1-p)\frac{\hat{I}_N - \hat{P}_N}{2^N - 2}, \tag{11}$$

with $\hat{P}_N = |\mathbf{0}_N\rangle\langle\mathbf{0}_N| + |\psi_N\rangle\langle\psi_N|$ denoting the projector onto the subspace formed by vectors $|\mathbf{0}_N\rangle$ and $|\psi_N\rangle$, and with $p = \text{Tr}\{\hat{P}_N\hat{\rho}_{\text{in}}\}$ denoting the probability with which the initial quantum state $\hat{\rho}_{\text{in}}$ has been prepared in this particular subspace. Due to the fact that all components of the initially prepared quantum state $\hat{\rho}_{\text{in}}$ inside this 2D subspace are not affected by the random unitary operations within the N-qubit quantum network, $\hat{P}_N$ projects onto an N-qubit decoherence free subspace. Furthermore, it is apparent from the structure of the attractors of theorem 3.1 that they are invariant under arbitrary permutations of qubits.

3.2. Attractor spaces of non-strongly connected interaction graphs

Theorem 3.1 states that the attractor spaces of quantum networks with a given conditional unitary two-qubit interaction (5) and with strongly connected interaction graphs are all identical. For non-strongly connected interaction graphs in general, the situation is much more complicated. In the following, we demonstrate that even these more general interaction graphs can be classified with respect to equivalence classes that share the same attractor space.

For this purpose it is convenient to partition a given non-strongly connected interaction graph $\mathsf{G}(\mathsf{V}, \mathsf{E})$ into all of its possible strongly connected subgraphs, say $\mathsf{G}_i(\mathsf{V}_i, \mathsf{E}_i)$, $i \in \{1, \ldots, r\}$. Such a partition is possible in a unique way because connectedness is an equivalence relation on the set of vertexes V of a graph $\mathsf{G}(\mathsf{V}, \mathsf{E})$ [23]. Thus, in each of these subgraphs (or dicomponents of continuity), any two vertexes are connected by some directed path in both directions. The so-called digraph of continuity $\mathfrak{G}$ [23] associated with the interaction graph $\mathsf{G}(\mathsf{V}, \mathsf{E})$ is a new graph whose vertexes are formed by the subgraphs $\mathsf{G}_i(\mathsf{V}_i, \mathsf{E}_i)$, $i \in \{1, \ldots, r\}$. Two vertexes of $\mathfrak{G}$, say $\mathsf{G}_i(\mathsf{V}_i, \mathsf{E}_i)$ and $\mathsf{G}_j(\mathsf{V}_j, \mathsf{E}_j)$, are connected by a directed edge if there is a directed edge in $\mathsf{G}(\mathsf{V}, \mathsf{E})$ whose tail lies in $\mathsf{G}_i(\mathsf{V}_i, \mathsf{E}_i)$ and whose head lies in $\mathsf{G}_j(\mathsf{V}_j, \mathsf{E}_j)$. Two non-strongly connected interaction graphs, say $\mathsf{G}(\mathsf{V}, \mathsf{E})$ and $\mathsf{H}(\mathsf{V}, \mathsf{E})$, are said to have equivalent digraphs of continuity, $\mathfrak{G}$ and $\mathfrak{H}$, if these digraphs of continuity are identical and if the vertexes of these digraphs of continuity correspond to the same vertexes of the associated non-strongly connected interaction graphs $\mathsf{G}(\mathsf{V}, \mathsf{E})$ and $\mathsf{H}(\mathsf{V}, \mathsf{E})$.

In terms of digraphs of continuity associated with non-strongly connected interaction graphs, the following general relation between their attractor spaces can be established:

Theorem 3.2. *Let* G *and* H *be two interaction graphs of N qubits with the same conditional unitary two-qubit interaction (5). If their corresponding digraphs of continuity* $\mathfrak{G}$ *and* $\mathfrak{H}$ *are equivalent, their attractor spaces are identical.*

This theorem tells us that for conditional unitary two-qubit interactions given by (5), even in the case of non-strongly connected interaction graphs, an attractor space depends only on the associated digraph of continuity and on the sets of qubits that constitute its vertexes. In particular, this implies that details of the coupling between qubits within a particular strongly connected subgraph or even some of the details of the qubit couplings between different strongly connected subgraphs are irrelevant to its attractor space. Thus, this theorem simplifies significantly the determination of attractor spaces of quantum networks randomly coupled by a conditional unitary two-qubit interaction (5) by characterizing completely which details of a given interaction graph are relevant for the asymptotic dynamics and which ones are irrelevant. Despite these simplifications, however, for large numbers of qubits, the set of all possible non-equivalent digraphs of continuity is still large.

For the proof of this theorem, we start from the observation that according to theorem 3.1, it is true for strongly connected interaction graphs. So, let us consider an interaction graph $\mathsf{G}(\mathsf{V}, \mathsf{E})$ that has two strongly connected subgraphs $\mathsf{G}_1(\mathsf{V}_1, \mathsf{E}_1)$ and $\mathsf{G}_2(\mathsf{V}_2, \mathsf{E}_2)$, and that involves a conditional unitary two-qubit interaction (5). The proof of more general cases is analogous. Let us denote the attractor spaces of these strongly connected subgraphs by Atr_1, Atr_2. Each of these attractor spaces does not depend on how qubits are connected within its associated subgraph. The only aspect that matters is that each subgraph is strongly connected. An arbitrary attractor $\hat{X}$ of the interaction graph $\mathsf{G}(\mathsf{V}, \mathsf{E})$ can be written as a linear combination in the form $\hat{X} = \sum_{ij} \alpha_{ij} \hat{X}_i^{(1)} \otimes \hat{X}_j^{(2)}$ with $\hat{X}_i^{(m)} \in \mathsf{Atr}_m$, $m \in \{1, 2\}$. The possible values of the coefficients α_{ij} are determined by the edges of the digraph of continuity. The attractors $\hat{X}_i^{(m)}$ are associated with the strongly connected subgraphs $\mathsf{G}_m(\mathsf{V}_m, \mathsf{E}_m)$. Therefore, they are symmetric with respect to arbitrary permutations of qubits within each subgraph. In particular, it does not matter which qubit is the control and which one the target. As a consequence, the attractor space of the interaction graph $\mathsf{G}(\mathsf{V}, \mathsf{E})$ depends only on the corresponding digraph of continuity and the vertexes of $\mathsf{G}(\mathsf{V}, \mathsf{E})$ constituting its own vertexes. This completes the proof of theorem 3.2. □

4. Asymptotic dynamics of open qubit networks in qubit environments of arbitrary sizes

An interesting property of the controlled unitary transformations (5) is their ability to create entanglement between qubits. Thus, the asymptotic dynamics of a qubit network governed by such randomly applied controlled unitary transformations is characterized by two competing mechanisms. On the one hand, the unitary two-qubit couplings tend to create coherence and entanglement within the qubit network; on the other hand, the classical randomness involved tends to destroy these characteristic quantum phenomena. Therefore, investigating the asymptotic dynamics of open subsystems of such quantum networks under large numbers of iterations offers the possibility of exploring intricate details of the interplay between these two competing mechanisms and their resulting influence on characteristic features, such as the

entropy exchange between an open quantum system and its environment. This entropy exchange is particularly interesting because, depending on the interaction topology, a subsystem of a qubit network may be cooled locally by an appropriate entropy exchange with its environment although in general random unitary transformations never decrease the total entropy of a qubit network [19, 20]. In order to examine the dependence of local entropy changes on the interaction topology, we investigate two different classes of open qubit subsystems in this section, namely subsystems that are part of a quantum network with a strongly connected interaction graph and subsystems that are part of a network with a non-strongly connected interaction graph in which the environmental qubits act as control qubits on the open subsystem.

4.1. Subsystem of a strongly connected qubit network

Let us consider a qubit network consisting of $(K+N)$ qubits that are coupled by randomly applied controlled unitary transformations (5) with $0<\phi<\pi$. We want to explore the asymptotic dynamics of an open subsystem of this qubit network, which is formed by K arbitrarily chosen qubits and whose dynamical properties are determined by the residual N qubits that constitute its finitely sized environment. For this purpose, we assume that the interaction graph characterizing the interaction topology of the total qubit network is strongly connected so that its attractor space is given by (8) and (10). Accordingly, the asymptotic quantum state of the total $(K+N)$-qubit network has the form (11).

In the limit of large environments, i.e. $N\gg 1$, the approximation $|\psi_{K+N}\rangle \longrightarrow |V_{k+N}\rangle(1+O(\cos^N(\phi/2)))$ is obtained with $|V_{K+N}\rangle=[(\cos(\phi/2)|0\rangle+\sin(\phi/2)|1\rangle)/\sqrt{2}]^{\otimes K+N}$. Thus, the resulting asymptotic quantum state of the K-qubit subsystem is given by

$$\hat{\rho}_\infty^{(S)}=p_V|V_K\rangle\langle V_K|+p_0|\mathbf{0}_K\rangle\langle\mathbf{0}_K|+(1-p_V-p_0)\frac{\hat{I}_K}{2^K}, \tag{12}$$

with the pure K-qubit quantum state $|\mathbf{0}_K\rangle=|0\rangle^{\otimes K}$. The sum of the probabilities $p_0=\langle\mathbf{0}_{K+N}|\hat{\rho}_{\mathrm{in}}|\mathbf{0}_{K+N}\rangle$ and $p_V=\langle V_{K+N}|\hat{\rho}_{\mathrm{in}}|V_{K+N}\rangle$ determines the overlap of the initially prepared quantum state $\hat{\rho}_{\mathrm{in}}$ with the $(K+N)$-qubit decoherence free subspace $\hat{P}_{K+N}$ defined by (11).

We may obtain additional insights into the consequences of equation (12) by considering initially uncorrelated quantum states between the subsystem and the environment of the form $\hat{\rho}_{\mathrm{in}}=\hat{\rho}^{(S)}\otimes\hat{\xi}^{\otimes N}$. For these initial states and for large values of N, the probabilities p_0 and p_V tend to zero unless $\hat{\xi}=|V_1\rangle\langle V_1|$ or $\hat{\xi}=|\mathbf{0}_1\rangle\langle\mathbf{0}_1|$. Therefore, independent of the initially prepared state $\hat{\rho}^{(S)}$, equation (12) yields, up to an exponentially small term, a maximally mixed state for the subsystem, i.e.

$$\hat{\rho}_\infty^{(S)}=\frac{\hat{I}_K}{2^K}, \tag{13}$$

for $p_0,\ p_V\to 0$. A special example of such a case is thermalization, i.e. maximization of the entropy of the subsystem, which occurs if the N environmental qubits are prepared in the maximally mixed state, i.e. $\hat{\xi}=\hat{I}_1/2$.

However, if initially the environment is prepared in the pure state $\hat{\xi}^{\otimes N}=|V_N\rangle\langle V_N|$, the resulting asymptotic quantum state of the subsystem assumes the form

$$\hat{\rho}_\infty^{(S)}=p|V_K\rangle\langle V_K|+(1-p)\frac{\hat{I}_K}{2^K}, \tag{14}$$

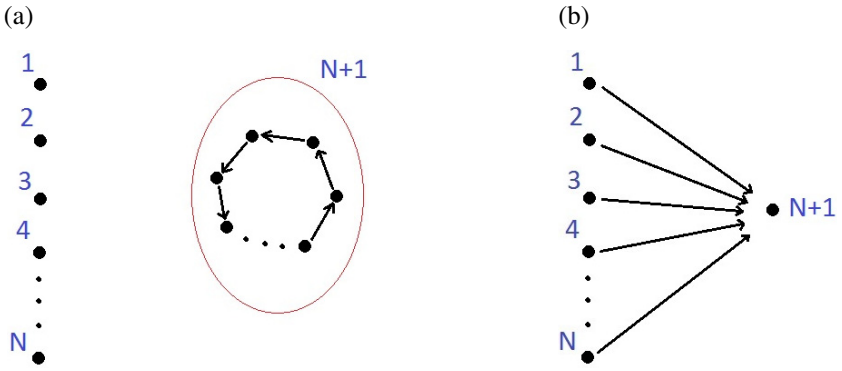

Figure 3. The $N+1$ strongly connected subgraphs or dicomponents of continuity $\mathsf{G}_i(\mathsf{V}_i, \mathsf{E}_i)$ $(i = 1, \ldots, N+1)$ (figure 3(a)) of the non-strongly connected interaction graph $\mathsf{G}(\mathsf{V}, \mathsf{E})$ of figure 1 are the vertexes of the associated digraph of continuity $\mathfrak{G}$ (figure 3(b)). Any directed edge between two vertexes of $\mathfrak{G}$ hints at the fact that according to the non-strongly connected interaction graph $\mathsf{G}(\mathsf{V}, \mathsf{E})$ of figure 1 there is a directed edge between the corresponding strongly connected subgraphs $\mathsf{G}_i(\mathsf{V}_i, \mathsf{E}_i)$.

with $p = \langle V_K|\hat{\rho}^{(S)}|V_K\rangle = p_V$. An analogous expression is obtained if the environment is prepared in the pure state $\hat{\xi}^{\otimes N} = |\mathbf{0}_N\rangle\langle\mathbf{0}_N|$ initially. In these cases, entropy can be extracted from the subsystem for some initially prepared quantum states $\hat{\rho}^{(S)}$ with $p > 0$ so that the environment can act as a 'refrigerator'. This is particularly apparent if the initial quantum state of the system is maximally mixed, i.e. $\hat{\rho}^{(S)} = \hat{I}_K/2^K$ so that $p = 2^{-K}$. Even more generally, it is straightforward to demonstrate that for a given value of K, the maximum amount of cooling is achieved for an initially prepared quantum state,

$$\hat{\rho}^{(S)} = p_{\max}|V_K\rangle\langle V_K| + (1 - p_{\max})\frac{\hat{I}_K^{\perp}}{2^K - 1}, \tag{15}$$

with $\hat{I}_K^{\perp}/(2^K - 1)$ denoting the maximally mixed state in the K-qubit subspace orthogonal to state $|V_K\rangle$ and with the mixing probability $p_{\max}$ being determined by the relation

$$\left(1 + \frac{1}{dp_{\max}}\right)^d (1 - p_{\max}) = dp_{\max}, \tag{16}$$

with $d = (2^K - 1)$. After larger numbers of random unitary transformations, this initially prepared quantum state is transformed into the asymptotic quantum state (14) with $p = p_{\max}$. The corresponding entropies and their dependence on the number of qubits of the subsystem K are depicted in figure 4. It is apparent that the entropy exchange between the subsystem and the environment decreases with increasing size of the subsystem.

In order to investigate the influence of the size of the environment on the entropy exchange between a K-qubit subsystem and its environment, let us consider the interesting case of a one-qubit subsystem with an initially prepared quantum state $\hat{\rho}_{\text{in}} = \hat{\rho}^{(S)} \otimes |V_N\rangle\langle V_N|$. The resulting entropy exchange depends not only on the initially prepared one-qubit quantum state $\hat{\rho}^{(S)}$ but also on the size of the environment N and on the controlled unitary coupling between the qubits, which is characterized by the parameter $0 < \phi < \pi$.

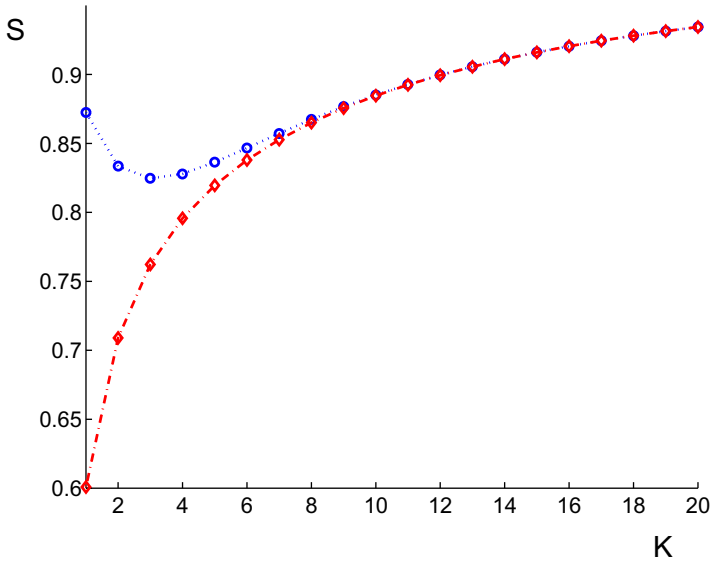

Figure 4. von Neumann entropies per qubit (in units of bits) of the quantum states (15) ($\cdots\cdots$, $\circ$, blue) and (14) ($—\cdot—$, $\diamondsuit$, red) and their dependence on the number of qubits K of the subsystem for $\hat{\xi} = |V_1\rangle\langle V_1|$, the optimal cooling effect achieved by large environments for $p_{\max}$ fulfilling (16) decreases with increasing size of the subsystem.

Let us first of all restrict our discussion to controlled-NOT operations, i.e. $\phi = \pi/2$. The dependence of the von Neumann entropy of the asymptotic quantum state $\hat{\rho}_{\infty}^{(S)}$ on the number of qubits of the environment N is depicted in figure 5 for different initially prepared quantum states with $\hat{\xi} = |V_1\rangle\langle V_1|$. It is straightforward to demonstrate that the only case for which the asymptotic von Neumann entropy is independent of the size of the environment arises for the initial state $\hat{\rho}^{(S)} = |V_1\rangle\langle V_1|$. Similarly, a strictly monotonically increasing dependence of the von Neumann entropy is obtained only for an initial state $\hat{\rho}^{(S)} = |V_1^{\perp}\rangle\langle V_1^{\perp}|$ with $\langle V_1|V_1^{\perp}\rangle = 0$. In all other cases, the von Neumann entropy is either strictly monotonically decreasing or it exhibits a single maximum whose position depends on the initially prepared quantum state $\hat{\rho}^{(S)}$. In these latter generic cases, sufficiently small environments increase the entropy of the one-qubit subsystem. For a critical size of the environment, this heating effect is maximal. For larger environments, this heating effect decreases again monotonically with increasing value of N.

These size-dependent heating and cooling effects become even more involved for controlled unitary transformations with $0 < \phi < \pi$. Typical resulting N dependences of asymptotic von Neumann entropies are depicted in figure 6 for different controlled unitary transformations and for $\hat{\xi} = |V_1\rangle\langle V_1|$. It is apparent that these N dependences of the asymptotic von Neumann entropy can even exhibit both a maximum and a minimum so that there are two critical sizes of the environment, namely one at which maximum heating occurs and another at which maximal cooling is achieved.

Let us finally consider cases in which the environment is not prepared in one of the exceptional quantum states $|V_N\rangle$ or $|\mathbf{0}_N\rangle$, which may achieve cooling even in the limit of large environments. For this purpose, let us consider cases in which the environment is prepared in a

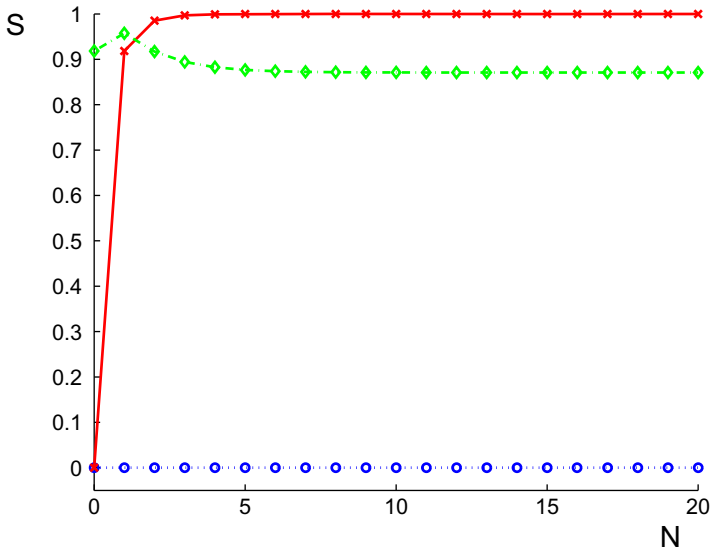

Figure 5. Asymptotic von Neumann entropy (in units of bits) and its dependence on the size N of the environment for different initial one-qubit states: $\hat{\rho}^{(S)} = |V_1\rangle\langle V_1|$ ($\cdots\cdots$, $\circ$, blue); $\hat{\rho}^{(S)} = |V_1^{\perp}\rangle\langle V_1^{\perp}|$ (——, $\times$, red); $\rho^{(S)} = p_\delta|\delta\rangle\langle\delta| + (1 - p_\delta)\hat{I}_1/2$ with $|\delta\rangle = (|0\rangle + e^{i\delta}|1\rangle)/\sqrt{2}$ and with $\delta = 2\pi/3$, $p_\delta = 1/3$ (— · —, $\Diamond$, green).

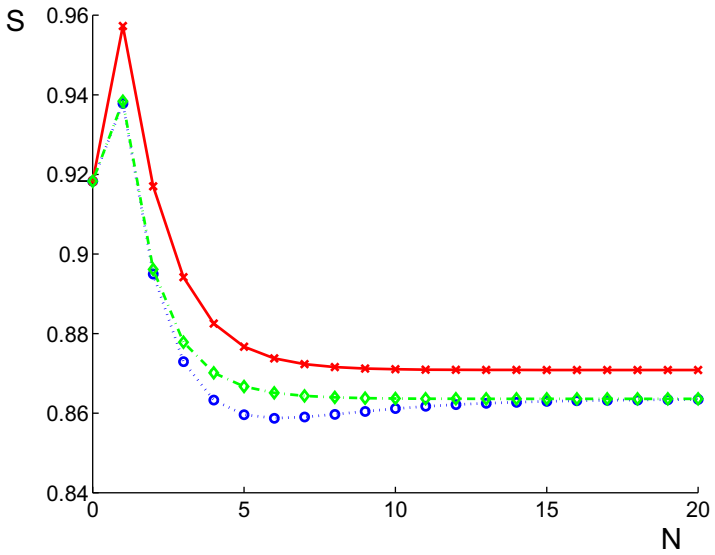

Figure 6. Asymptotic von Neumann entropy (in units of bits) and its dependence on the size of the environment N for initial one-qubit states $\rho^{(S)} = p_\delta|\delta\rangle\langle\delta| + (1 - p_\delta)\hat{I}_1/2$, $|\delta\rangle = (|0\rangle + e^{i\delta}|1\rangle)/\sqrt{2}$, $\delta = 2\pi/3$, $p_\delta = 1/3$ and for different controlled unitary transformations: $\phi = \pi/3$ ($\cdots\cdots$, $\circ$, blue), $\phi = \pi/2$ (——, $\times$, red), $\phi = 2\pi/3$ (— · —, $\Diamond$, green).

quantum state $\hat{\xi}^{\otimes N}$ with

$$\hat{\xi} = (1 - \epsilon)|V_1\rangle\langle V_1| + \epsilon\frac{\hat{I}_1}{2}. \tag{17}$$

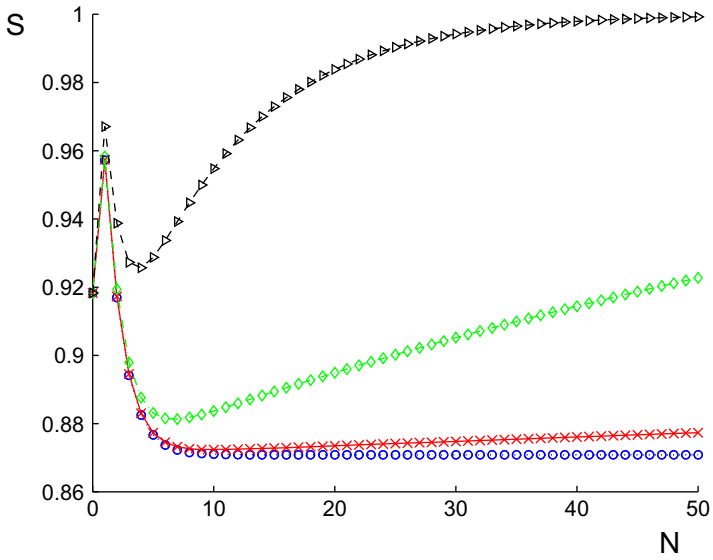

Figure 7. Asymptotic von Neumann entropy (in units of bits) and its dependence on the size of the environment N for different initial environmental states $\hat{\xi}^{\otimes N}$ with $\hat{\xi}$ as defined by (17): $\epsilon = 0$ ($\circ$, blue), $\epsilon = 0.001$ ($\times$, red), $\epsilon = 0.01$ ($\diamondsuit$, green) and $\epsilon = 0.1$ ($\triangle$, black).

The corresponding N dependence of the asymptotic von Neumann entropy is depicted in figure 7 for different values of ϵ and for an initial one-qubit state $\rho^{(S)} = p_\delta|\delta\rangle\langle\delta| + (1 - p_\delta)\hat{I}_1/2$ with $|\delta\rangle = (|0\rangle + e^{i\delta}|1\rangle)/\sqrt{2}$ and with $\delta = 2\pi/3$, $p_\delta = 1/3$. It is apparent that with increasing deviation of the initially prepared state of the environment from $\hat{\xi}^{\otimes N} = |V_N\rangle\langle V_N|$, the asymptotic cooling effect decreases so that eventually cooling can be achieved only for sufficiently small numbers of environmental qubits.

4.2. Subsystem of a non-strongly connected qubit network

In order to investigate the influence of the interaction topology on the entropy transport within a quantum network, let us now consider interaction graphs that are non-strongly connected. In particular, let us focus on cases in which the open K-qubit subsystem is described by a strongly connected interaction graph and in which these K qubits couple in a random way as target qubits to its N environmental qubits that constitute the control qubits. An example of such an interaction topology is depicted in figure 1. For the sake of simplicity, let us first of all neglect direct couplings between the environmental qubits. Later in this section, this restriction will be relaxed and it will be shown that the way in which the environmental qubits are coupled among themselves has no influence on the resulting asymptotic dynamics of the open system. This remarkable observation indicates that, as far as the asymptotic dynamics of the subsystem are concerned, there are relevant and irrelevant properties beyond the concept of the digraph of continuity that characterize the asymptotic dynamics of the whole network.

As the interaction graph of the total $(K + N)$-qubit system is not strongly connected, theorem 3.2 applies. This theorem tells us that in the asymptotic limit of large numbers of iterations, the state of the complete quantum network is determined uniquely by the relevant digraph of continuity, which is depicted in figure 3(b) for the interaction graph of figure 1. In particular, this implies that this asymptotic quantum state is independent of the detailed

form of the strongly connected interaction graph of the K-qubit subsystem. Furthermore, details concerning which environmental qubit couples to which qubit of the open K-qubit subsystem are also irrelevant. This irrelevance is reflected in the fact that in the digraph of continuity, each strongly connected part of the interaction graph collapses to a vertex and the directed edges of the digraph of continuity do not contain information as to which qubits of different strongly connected subgraphs are connected in the original interaction graph. As a consequence, the digraph of continuity of this $(K+N)$-qubit quantum network has $(N+1)$ components. One of them is formed by the strongly connected interaction graph of the open K-qubit subsystem. Each of the environmental qubits forms a trivial strongly connected subgraph of its own because all couplings in which environmental qubits are target qubits are neglected for the moment. They are taken into account later in this section, where it will be shown that they do not alter our conclusions concerning the open K-qubit subsystem.

Let us now determine the asymptotic quantum state resulting from an initially uncorrelated quantum state $\hat{\rho}_{\mathrm{in}} = \hat{\rho}^{(S)} \otimes \hat{\rho}^{(E)}$ of the K-qubit subsystem and its N-qubit environment $(K + N \geqslant 3)$. For this purpose, we have to determine an orthonormal basis of the attractor space of the non-strongly connected interaction graph of figure 1. When solving the eigenvalue equations (2), it turns out that the attractor space of this $(K+N)$-qubit system is $(4^N + 3 \cdot 2^N + 1)$-dimensional, that the only possible eigenvalue is given by $\lambda = 1$ and that an orthonormal basis system of attractors is given by

$$\begin{aligned}
&\hat{X}_i \otimes |\mathbf{0}_N\rangle\langle\mathbf{0}_N|, \quad |\mathbf{0}_K\rangle\langle V_K| \otimes |\mathbf{0}_N\rangle\langle \boldsymbol{y}|,\\
&|\psi_K\rangle\langle V_K| \otimes |\mathbf{0}_N\rangle\langle \boldsymbol{y}|, \quad |V_K\rangle\langle\mathbf{0}_K| \otimes |\boldsymbol{y}\rangle\langle\mathbf{0}_N|,\\
&|V_K\rangle\langle\psi_K| \otimes |\boldsymbol{y}\rangle\langle\mathbf{0}_N|, \quad |V_K\rangle\langle V_K| \otimes |\boldsymbol{y}\rangle\langle\boldsymbol{y}|,\\
&|V_K\rangle\langle V_K| \otimes |\boldsymbol{y}\rangle\langle\boldsymbol{z}|, \quad \frac{1}{\sqrt{2^K-1}}(\hat{I}_K - |V_K\rangle\langle V_K|) \otimes |\boldsymbol{y}\rangle\langle\boldsymbol{y}|,
\end{aligned} \tag{18}$$

with $i \in \{1, 2, \ldots, 5\}, 0 \neq \boldsymbol{y} \in \mathsf{I}_N, 0 \neq \boldsymbol{z} \in \mathsf{I}_N$. Thereby, the first parts of the tensor products refer to the K-qubit subsystem and the second parts to the N-qubit environment. The pure K-qubit quantum states $|\psi_K\rangle$ and $|V_K\rangle$ are defined in (9) and (12). By tracing out the environment, we finally obtain the asymptotic stationary quantum state of the K-qubit subsystem, i.e.

$$\hat{\rho}^{(S)}_{\infty} = p^{(0)}_{\mathrm{env}} \hat{\rho}^{(S)}_0 + (1 - p^{(0)}_{\mathrm{env}}) \hat{\rho}^{(S)}_1, \tag{19}$$

with $p^{(0)}_{\mathrm{env}}$ denoting the probability with which the environment was prepared initially in state $|\mathbf{0}_N\rangle$. This probability is the only parameter of the environment that enters the asymptotic state of the K-qubit subsystem. According to (19), the asymptotic quantum state of the interaction center is a convex sum of the two states

$$\begin{aligned}
\hat{\rho}^{(S)}_0 &= \sum_{i=1}^{5} \mathrm{Tr}\{\hat{\rho}^{(S)} \hat{X}_i^{\dagger}\} \hat{X}_i,\\
\hat{\rho}^{(S)}_1 &= \langle V_K|\hat{\rho}^{(S)}|V_K\rangle |V_K\rangle\langle V_K| + (1 - \langle V_K|\hat{\rho}^{(S)}|V_K\rangle) \frac{\hat{I}^{\perp}_K}{2^K - 1}.
\end{aligned} \tag{20}$$

Thereby, $\hat{\rho}^{(S)}_0$ characterizes all quantum features of the K-qubit subsystem that are not affected by the conditional unitary coupling to the environment. In view of the random couplings among the qubits of this open subsystem, this quantum state can be entangled even if the initially prepared quantum state $\hat{\rho}^{(S)}$ of the K-qubit subsystem is separable. But apparently the quantum

state $\hat{\rho}_1^{(S)}$ is always separable with respect to arbitrary partitions of the K-qubit subsystem. Therefore, the transformation between the initial quantum state $\hat{\rho}^{(S)}$ and the final quantum state (19) is entanglement breaking.

For initially prepared environmental quantum states $\hat{\rho}^{(E)} = \hat{\xi}^{\otimes N}$ and for large environments with $N \gg 1$, two different cases can arise. If $\hat{\xi} = |\mathbf{0}_1\rangle\langle\mathbf{0}_1|$, the probability $p_{\mathrm{env}}^{(0)}$ equals unity so that the asymptotic quantum state is given by $\hat{\rho}_0^{(S)}$. Thus, the environment does not influence the asymptotic quantum state at all. However, if $0 \leqslant \langle\mathbf{0}_1|\hat{\xi}|\mathbf{0}_1\rangle < 1$, the probability $p_{\mathrm{env}}^{(0)} = \langle\mathbf{0}_1|\hat{\xi}|\mathbf{0}_1\rangle^N$ tends to zero so that the asymptotic quantum state of the K-qubit subsystem is given by the separable quantum state $\hat{\rho}_1^{(S)}$ of the form (20). In view of this fact, we conclude that this quantum network makes the process of thermalization, i.e. maximization of the entropy of the subsystem, impossible.

The transformation of any initial quantum state $\hat{\rho}^{(S)}$ to this final state can also be viewed as arising from a two-step process involving a projective von Neumann measurement with the projection operator $|V_K\rangle\langle V_K|$ and a second quantum operation that transforms the orthogonal component of the initial state into the maximally mixed state $\hat{I}_K^{\perp}/(2^K - 1)$. Definitely, these quantum operations do not decrease the entropy of any initially prepared quantum state $\hat{\rho}^{(S)}$, so that cooling of the K-qubit subsystem is impossible in such a qubit network. This impossibility may be traced back to the fact that in such a quantum network the qubits of the K-qubit subsystem act as target qubits only as far as the coupling between the open subsystem and its environment is concerned.

Also, in the case of a finite environment with an arbitrary value of $p_{\mathrm{env}}^{(0)}$, the entropy of the asymptotic quantum state (19) cannot be smaller than the von Neumann entropy of an arbitrary initially prepared quantum state $\hat{\rho}^{(S)}$. This can be seen from the inequalities

$$\begin{aligned} S(\hat{\rho}_{\infty}^{(S)}) &\geqslant p_{\mathrm{env}}^{(0)} S(\hat{\rho}_0^{(S)}) + (1 - p_{\mathrm{env}}^{(0)}) S(\hat{\rho}_1^{(S)}) \\ &\geqslant p_{\mathrm{env}}^{(0)} S(\hat{\rho}^{(S)}) + (1 - p_{\mathrm{env}}^{(0)}) S(\hat{\rho}^{(S)}) = S(\hat{\rho}^{(S)}). \end{aligned} \tag{21}$$

The first inequality of (21) reflects the mixing property of the von Neumann entropy. The second inequality takes into account the fact that random unitary transformations cannot decrease the von Neumann entropy, i.e. $S(\hat{\rho}_0^{(S)}) \geqslant S(\hat{\rho}^{(S)})$, and that $S(\hat{\rho}_1^{(S)}) \geqslant S(\hat{\rho}^{(S)})$, as was shown in the previous paragraph. Thus, in general, the K-qubit subsystem cannot be cooled in such a quantum network.

Let us focus now on the question of how random conditional unitary couplings between environmental qubits influence the asymptotic dynamics of the K-qubit subsystem. Surprisingly, although in general such additional purely environmental couplings change the asymptotic quantum state of the complete $(K + N)$-qubit system, these couplings do not at all affect the asymptotic quantum state of the K-qubit subsystem. In the asymptotic regime, the open subsystem does not undergo any changes in the environmental couplings no matter whether the initial state of the open system and its environment is separable or entangled. This surprising result is partly a further consequence of our main theorems 3.1 and 3.2 and partly reflects some additional characteristic properties of randomly interacting quantum networks whose two-qubit interactions are given by (5). However, a systematic investigation of these properties is outside the scope of this paper and will be given elsewhere. Thus, all previously derived results of this section are valid, irrespective of whether environmental qubits are interacting or not.

The proof of this general feature is surprisingly simple and involves two main steps. In the first step, one demonstrates that the asymptotic dynamics of the K-qubit subsystem do

not change in those extreme cases where the environmental qubits are all coupled among themselves so that the interaction graph of the environment g_1 is completely connected. This is the extreme opposite limit of the previously investigated non-interacting situation. In this case, the interaction graph of the total $(K+N)$-qubit system, G_1, has only two dicomponents of continuity and the attractor space of the associated digraph of continuity turns out to be 12D. An orthonormal basis of this attractor space is given by

$$\begin{aligned}
&\hat{X}_i \otimes |\mathbf{0}_N\rangle\langle\mathbf{0}_N|, \quad |\mathbf{0}_K\rangle\langle V_K| \otimes |\mathbf{0}_N\rangle\langle\psi_N|,\\
&|\psi_K\rangle\langle V_K| \otimes |\mathbf{0}_N\rangle\langle\psi_N|, \quad |V_K\rangle\langle\mathbf{0}_K| \otimes |\psi_N\rangle\langle\mathbf{0}_N|,\\
&|V_K\rangle\langle\psi_K| \otimes |\psi_N\rangle\langle\mathbf{0}_N|, \quad |V_K\rangle\langle V_K| \otimes |\psi_N\rangle\langle\psi_N|,\\
&\frac{|V_K\rangle\langle V_K|}{\sqrt{2^N-2}} \otimes (\hat{I}_N - |\mathbf{0}_N\rangle\langle\mathbf{0}_N| - |\psi_N\rangle\langle\psi_N|),\\
&\frac{(I_K - |V_K\rangle\langle V_K|)}{\sqrt{(2^N-2)(2^K-1)}} \otimes (\hat{I}_N - |\mathbf{0}_N\rangle\langle\mathbf{0}_N|).
\end{aligned} \tag{22}$$

Determining the asymptotic quantum state of the K-qubit subsystem with the help of these attractors, we obtain the same result as in (19).

In the second step of the proof, we consider also cases where not all of the qubit pairs of the environment interact with each other. Let g be the environmental interaction graph of such a case and G the corresponding interaction graph of the N-qubit environment and the K-qubit subsystem. Denoting the interaction graphs of a non-interacting environment and of the corresponding K-qubit subsystem by g_2 and G_2, respectively, the relation

$$\mathsf{g}_1 \subseteq \mathsf{g} \subseteq \mathsf{g}_2 \tag{23}$$

holds. According to relation (4), the corresponding attractor spaces of these three cases satisfy the relation

$$\mathsf{Atr}_{\mathsf{g}_2} \subseteq \mathsf{Atr}_{\mathsf{g}} \subseteq \mathsf{Atr}_{\mathsf{g}_1}. \tag{24}$$

This allows us to choose orthonormal bases in these attractor spaces in the following way. Firstly, we choose an orthonormal basis $\{\hat{r}_i\}$ of $\mathsf{Atr}_{\mathsf{g}_2}$, afterwards an orthonormal basis $\{\hat{r}_i, \hat{s}_j\}$ of $\mathsf{Atr}_{\mathsf{g}}$ and finally an orthonormal basis $\{\hat{r}_i, \hat{s}_j, \hat{t}_k\}$ of $\mathsf{Atr}_{\mathsf{g}_1}$ with appropriate ranges of indices. Starting from these basis elements, we can construct orthonormal bases of the corresponding complete quantum systems with the help of tensor products between basis states of the attractors of the N-qubit environment and of the K-qubit subsystem. Thereby, one has to take into account that the couplings between these two parts of the quantum network impose constraints on possible attractors of the total $(K+N)$-qubit system. At this point, it is important to remember that according to our system–reservoir model, all edges between the N-qubit environment and the K-qubit subsystem start in the environment because all environmental qubits are control qubits as far as the coupling to the K-qubit subsystem is concerned. As a result, we can choose the basis states of the attractor space of the total $(K+N)$-qubit quantum system in the following way. The orthonormal basis of $\mathsf{Atr}_{\mathsf{G}_2}$ is of the form $\{\hat{r}^1_{i_1} \otimes \hat{R}^{i_1}_{u_{i_1}}\}$. This notation reflects the fact that this basis is constructed by taking a basis element of the environmental attractor space, say $\hat{r}_i$, and finding a basis, say $\{\hat{R}^i_{u_i}\}$, for all possible attractors of the K-qubit subsystem that is consistent with the conditions imposed by the edges leading from the environment to

the K-qubit subsystem. Repeating this procedure for all basis elements of the environmental attractor space yields the orthonormal basis $\{\hat{r}^1_{i_1} \otimes \hat{R}^{i_1}_{u_{i_1}}\}$ of the total quantum system. Thereby, the introduction of the double indices takes into account that there are some basis elements $\hat{r}_i$ of the environmental attractor space for which no attractor of the K-qubit subsystem can be found or for which the corresponding attractor space of the K-qubit subsystem is more than 1D. The set $\{\hat{r}^1_{i_1}\}$ is the particular subset of orthonormal environmental basis elements $\{\hat{r}_i\}$ for which solutions exist. They are indexed by i_1 and the corresponding solutions of the K-qubit subsystem are indexed by u_{i_1}. Naturally, all of the attractors of the graph G_2 are also attractors of the interaction graphs G and G_1. Hence, we include them in the construction of their attractor spaces. Thus, analogously orthonormal basis systems of the attractor spaces of the interaction graphs G and G_1 are of the form $\{\hat{r}^1_{i_1} \otimes \hat{R}^{i_1}_{u_{i_1}}, \hat{r}^2_{i_2} \otimes \hat{R}^{i_2}_{u_{i_2}}, \hat{s}^1_{j_1} \otimes \hat{S}^{j_1}_{v_{j_1}}\}$ and $\{\hat{r}^1_{i_1} \otimes \hat{R}^{i_1}_{u_{i_1}}, \hat{r}^2_{i_2} \otimes \hat{R}^{i_2}_{u_{i_2}}, \hat{r}^3_{i_3} \otimes \hat{R}^{i_3}_{u_{i_3}}, \hat{s}^1_{j_1} \otimes \hat{S}^{j_1}_{v_{j_1}}, \hat{s}^2_{j_2} \otimes \hat{S}^{j_2}_{v_{j_2}}, \hat{t}^1_{k_1} \otimes \hat{T}^{k_1}_{w_{k_1}}\}$.

With the help of these orthonormal bases and of equation (3), the asymptotic quantum states of the K-qubit subsystem for the three interaction graphs G_1, G and G_2 are given by

$$\hat{\rho}_{\infty,\mathsf{G}_2} = \sum_{i_1,u_{i_1}} \hat{R}^{i_1}_{u_{i_1}} \mathrm{Tr}\hat{r}^1_{i_1} \mathrm{Tr}((\hat{r}^1_{i_1})^\dagger \hat{\rho}_{\mathrm{env}}) \mathrm{Tr}((\hat{R}^{i_1}_{u_{i_1}})^\dagger \hat{\rho}_0),$$

$$\begin{aligned}\hat{\rho}_{\infty,\mathsf{G}} = &\sum_{a=1}^{2} \sum_{i_a,u_{i_a}} \hat{R}^{i_a}_{u_{i_a}} \mathrm{Tr}\hat{r}^a_{i_a} \mathrm{Tr}((\hat{r}^a_{i_a})^\dagger \hat{\rho}_{\mathrm{env}}) \mathrm{Tr}((\hat{R}^{i_a}_{u_{i_a}})^\dagger \hat{\rho}_0) \\ &+ \sum_{j_1,v_{j_1}} \hat{S}^{j_1}_{v_{j_1}} \mathrm{Tr}\hat{s}^1_{j_1} \mathrm{Tr}((\hat{s}^1_{j_1})^\dagger \hat{\rho}_{\mathrm{env}}) \mathrm{Tr}((\hat{S}^{j_1}_{v_{j_1}})^\dagger \hat{\rho}_0),\end{aligned}$$

$$\begin{aligned}\hat{\rho}_{\infty,\mathsf{G}_1} = &\sum_{a=1}^{3} \sum_{i_a,u_{i_a}} \hat{R}^{i_a}_{u_{i_a}} \mathrm{Tr}\hat{r}^a_{i_a} \mathrm{Tr}((\hat{r}^a_{i_a})^\dagger \hat{\rho}_{\mathrm{env}}) \mathrm{Tr}((\hat{R}^{i_a}_{u_{i_a}})^\dagger \hat{\rho}_0) \\ &+ \sum_{b=1}^{2} \sum_{j_b,v_{j_b}} \hat{S}^{j_b}_{v_{j_b}} \mathrm{Tr}\hat{s}^b_{j_b} \mathrm{Tr}((\hat{s}^b_{j_b})^\dagger \hat{\rho}_{\mathrm{env}}) \mathrm{Tr}((\hat{S}^{j_b}_{v_{j_b}})^\dagger \hat{\rho}_0) \\ &+ \sum_{k_1,w_{k_1}} \hat{T}^{k_1}_{w_{k_1}} \mathrm{Tr}\hat{t}^1_{k_1} \mathrm{Tr}((\hat{t}^1_{k_1})^\dagger \hat{\rho}_{\mathrm{env}}) \mathrm{Tr}((\hat{T}^{k_1}_{w_{k_1}})^\dagger \hat{\rho}_0). \qquad (25)\end{aligned}$$

We have already proved that $\hat{\rho}_{\infty,\mathsf{G}_2} = \hat{\rho}_{\infty,\mathsf{G}_1}$ for all initially prepared density operators $\hat{\rho}^{(E)}$ and $\hat{\rho}^{(S)}$. Hence, by subtraction we obtain the result

$$\begin{aligned}0 &= \hat{\rho}_{\infty,\mathsf{G}_1} - \hat{\rho}_{\infty,\mathsf{G}_2} \\ &= \sum_{a=2}^{3} \sum_{i_a,u_{i_a}} \hat{R}^{i_a}_{u_{i_a}} \mathrm{Tr}\hat{r}^a_{i_a} \mathrm{Tr}((\hat{r}^a_{i_a})^\dagger \hat{\rho}_{\mathrm{env}}) \mathrm{Tr}((\hat{R}^{i_a}_{u_{i_a}})^\dagger \hat{\rho}_0) \\ &\quad + \sum_{b=1}^{2} \sum_{j_b,v_{j_b}} \hat{S}^{j_b}_{v_{j_b}} \mathrm{Tr}\hat{s}^b_{j_b} \mathrm{Tr}((\hat{s}^b_{j_b})^\dagger \hat{\rho}_{\mathrm{env}}) \mathrm{Tr}((\hat{S}^{j_b}_{v_{j_b}})^\dagger \hat{\rho}_0) \\ &\quad + \sum_{k_1,w_{k_1}} \hat{T}^{k_1}_{w_{k_1}} \mathrm{Tr}\hat{t}^1_{k_1} \mathrm{Tr}((\hat{t}^1_{k_1})^\dagger \hat{\rho}_{\mathrm{env}}) \mathrm{Tr}((\hat{T}^{k_1}_{w_{k_1}})^\dagger \hat{\rho}_0). \qquad (26)\end{aligned}$$

Finally, by appropriate choice of the density operators $\hat{\rho}^{(E)}$ and $\hat{\rho}^{(S)}$, it is straightforward to show that all operators $\{\hat{r}^2_{i_2}\}$, $\{\hat{r}^3_{i_3}\}$, $\{\hat{s}^1_{j_1}\}$, $\{\hat{s}^2_{j_2}\}$, and $\{\hat{t}^1_{k_1}\}$ have zero trace. As a direct consequence, we finally arrive at the equality

$$\hat{\rho}_{\infty,\mathsf{G}_2} = \hat{\rho}_{\infty,\mathsf{G}} = \hat{\rho}_{\infty,\mathsf{G}_1}. \tag{27}$$

It is important to emphasize that in the proof, we did not use the property that $\hat{\rho}_{\mathrm{env}}$ and $\hat{\rho}_0$ are density operators. In fact, this is not important and the last equation (27) holds for an arbitrary tensor product $\hat{A} \otimes \hat{B}$, with $\hat{A}$ ($\hat{B}$) being an operator acting on the K-qubit Hilbert space (N-qubit Hilbert space). An arbitrary initial state $\hat{\rho}_{\mathrm{in}}$ of the open system and its environment can be decomposed into a linear combination of terms in the tensor product form $\hat{A} \otimes \hat{B}$. Therefore, (27) holds for an arbitrary initial state $\hat{\rho}_{\mathrm{in}}$, which completes the proof. □

5. Conclusions

We have investigated the asymptotic dynamics of qubit networks of arbitrary size under the influence of repeatedly and randomly applied entangling unitary two-qubit operations within an exactly solvable model. General results have been derived for a particular one-parameter family of entanglement generating controlled unitary transformations in the form of two main theorems. They relate the topology of the interaction graph of a qubit network to its asymptotic dynamics. These two theorems state clearly those features of an interaction graph of a quantum network that are relevant for determining its asymptotic dynamics.

On the basis of these general results, the interplay between entanglement generation and classical randomness originating from uncontrolled applications of these entangling unitary transformations has been investigated. It has been demonstrated that although the overall entropy of such a quantum network cannot decrease, it is possible that subsystems lower their entropy locally and are thus cooled by entropy transport to their environment. In fact, both maximization, i.e. thermalization, and reduction, i.e. cooling, of the local entropy of a subsystem are possible if couplings between this subsystem and its environment act in both directions. If this condition is violated, successful realization of both processes is not possible. In particular, the possibility of local cooling hints at one of the surprising quantum features that can result from the competition between entanglement generation and classical randomness. Without invoking a Markov approximation or a weak coupling assumption, the dependence of this entropy exchange between a subsystem and its environment has been explored in the case of different topologies of interaction graphs and in the case of different sizes of the subsystem and its environment. For moderate numbers of qubits, these characteristic quantum effects should be amenable to further experimental exploration.

We have considered cases in which classical randomness is fed into a quantum network by selecting the entanglement generating unitary operations according to some arbitrarily chosen probability distribution that is held constant during the iteration process. It is found that the resulting asymptotic quantum state is independent of details of this probability distribution and that it depends only on its support, i.e. on the set of qubits that can be entangled at all by the unitary entanglement operation. This robustness of the asymptotic quantum state might offer advantages in experimental investigations of asymptotic network dynamics.

In addition to the ones investigated in this work, there are numerous other means of influencing the dynamics of a quantum system externally in a probabilistic way. One of them is information feedback based on quantum measurements [3]; another is decoherence by

decorrelation [24], for example. It might be of interest for future investigations to find links between the results presented in this work and more general forms of randomness-assisted quantum phenomena.

Acknowledgments

Financial support from the Alexander von Humboldt Foundation, CASED and MSM6840770039 and MSMT LC06002 of the Czech Republic is acknowledged.

Appendix. Attractor spaces of strongly connected interaction graphs

In this appendix, theorem 3.1 is proved in two main steps. In a first step, it is proved for the special case of qubit networks randomly coupled by controlled-NOT operations. The graph theoretical methods [23] used in this first step are used subsequently in a slightly modified form to prove theorem 3.1 also for general conditional unitary transformations described by (5).

A.1. Random qubit networks with controlled-NOT couplings

We construct an orthonormal basis system for the set of eigenvalue equations (2) for the special case of controlled-NOT operations defined by (5) with $\phi = \pi/2$ and for a completely connected interaction graph $\mathsf{G}(\mathsf{V}, \mathsf{E})$. These equations determine the minimal asymptotic attractor space. In addition, we have to demonstrate that strongly connected interaction graphs are the most general interaction graphs with the same minimal attractor space.

Because we are dealing with controlled-NOT operations, the possible eigenvalues can only assume the values $\lambda = 1$ or $\lambda = -1$. Let us denote the orthonormal basis states of the computational basis of N qubits by $|z\rangle$ with the binary N-tuples $z \equiv (z_1, z_2, \ldots, z_N) \in \{0, 1\}^N \equiv \mathsf{I}_N$. In this computational basis, an arbitrary linear operator in the Hilbert space of N qubits is given by

$$\hat{X} \equiv \sum_{\boldsymbol{i},\boldsymbol{j} \in \mathsf{I}_N} X_{(\boldsymbol{i},\boldsymbol{j})} |\boldsymbol{i}\rangle\langle\boldsymbol{j}| \tag{A.1}$$

and the eigenvalue equations (2) reduce to the form

$$X_{(\boldsymbol{i}',\boldsymbol{j}')} = \lambda X_{(\boldsymbol{i},\boldsymbol{j})} \tag{A.2}$$

with $\boldsymbol{i}' = (i_1, i_2, \ldots, i'_{\mathrm{t}} = i_{\mathrm{t}} \oplus i_{\mathrm{c}}, \ldots, i_N)$, $\boldsymbol{j}' = (j_1, j_2, \ldots, j'_{\mathrm{t}} = j_{\mathrm{t}} \oplus i_{\mathrm{c}}, \ldots, j_N)$ and with the subscripts t and c referring to the target and the control qubits, respectively. The symbol $\oplus$ denotes addition modulo two. Due to special properties of controlled-NOT operations, one can distinguish five subsets of all indices $(\boldsymbol{i}, \boldsymbol{j}) \in \mathsf{I}_N \times \mathsf{I}_N$ with the property that equations (A.2) do not couple matrix elements with indices from different subsets. These five subsets are given by

$$\begin{aligned} &\mathsf{A}_1 = \{(\boldsymbol{0}, \boldsymbol{0})\}, \quad \mathsf{A}_2 = \{(\boldsymbol{i}, \boldsymbol{0}) | \boldsymbol{i} \neq \boldsymbol{0}\}, \quad \mathsf{A}_3 = \{(\boldsymbol{0}, \boldsymbol{i}) | \boldsymbol{i} \neq \boldsymbol{0}\}, \\ &\mathsf{A}_4 = \{(\boldsymbol{i}, \boldsymbol{i}) | \boldsymbol{i} \neq \boldsymbol{0}\}, \quad \mathsf{A}_5 = \{(\boldsymbol{i}, \boldsymbol{j}) | \boldsymbol{i} \neq \boldsymbol{j} \neq \boldsymbol{0} \wedge \boldsymbol{i} \neq \boldsymbol{0}\}, \end{aligned} \tag{A.3}$$

with $\boldsymbol{0}$ denoting the zero vector of indices.

The couplings between the matrix elements of $\hat{X}$ can be encoded in a convenient way by an index graph $\mathsf{g}(\mathsf{I}, \mathsf{e})$, which is associated with an interaction graph $\mathsf{G}(\mathsf{V}, \mathsf{E})$. All members of

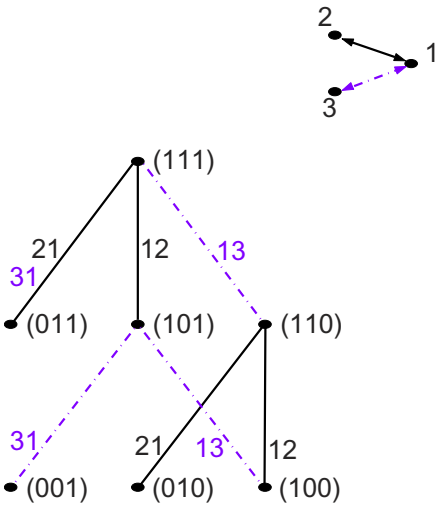

Figure A.1. Colored index graph (bottom) induced by a three-qubit oriented-star interaction graph (top): the index graph of the three qubits is formed by three dicomponents of continuity (bottom: solid lines and dot (001)), two of which are two-connected isomorphic index graphs of a two-qubit oriented-star interaction graph with a third qubit attached in state $|0\rangle$ and $|1\rangle$, respectively. The third component has only one vertex associated with the quantum state $|001\rangle$. These three dicomponents of continuity are connected by the colors 13 and 31 (bottom: dashed-dotted lines). The associated three-qubit star interaction graph is constructed from the two-qubit star interaction graph (top solid line) by attaching the third qubit as a vertex and by connecting it by an edge with the first qubit (top dashed-dotted line).

the index set I_N except for the element $\mathbf{0}$ are chosen as vertexes of such an index graph. This choice reflects the fact that the quantum state $|\mathbf{0}\rangle$ is trivial as it is not affected by controlled-NOT operations. Each edge $e \in \mathsf{E}$ of the interaction graph defines a 'colored' edge $\boldsymbol{ij}$ of the index graph with $\boldsymbol{j} = e\boldsymbol{i} \Leftrightarrow |\boldsymbol{j}\rangle = U_e|\boldsymbol{i}\rangle$ and with $\hat{U}_e$ denoting the appropriate controlled-NOT operation connecting these qubit states. The 'color' of this edge is denoted by e. Because of the property $e(e\boldsymbol{i}) = \boldsymbol{i}$, the index graph $\mathsf{g}(\mathsf{I}, \mathsf{e})$ is undirected. Each of its vertexes is the starting point of exactly m (colored) edges, with m denoting the total number of edges of the associated interaction graph. Thus, without loss of information, all loop-like edges with $e\boldsymbol{i} = \boldsymbol{i}$ need not be indicated explicitly in an index graph.

Following this convention, an example of an index graph induced by an interaction graph with three qubits is depicted in figure A.1.

A.1.1. The attractor space with $\lambda = 1$. Let us first consider the minimal attractor space with eigenvalue $\lambda = 1$. Definitely, this minimal attractor space arises in the case of a completely connected interaction graph. Considering the orthonormal basis given as (8) in the computational basis $\{|z\rangle\}$, one observes that we have to demonstrate that the minimal attractor space is formed by all $2^N \times 2^N$-matrices whose matrix elements are equal for indices $(\boldsymbol{i}, \boldsymbol{j})$ within the same index set A_l ($l \in \{1, \ldots, 5\}$) of (A.3). This property is always fulfilled trivially for the set A_1 because this set has only one element. Formulated in terms of the graph

theoretical concepts introduced, for the sets A_2, A_3 and A_4 it is true iff the index graph of a completely connected interaction graph is (one-) connected and for the set A_5 it is true iff this index graph is two-connected so that any pair of vertexes, say $(\boldsymbol{i}_1, \boldsymbol{j}_1)$, is connected to any other pair $(\boldsymbol{i}_2, \boldsymbol{j}_2)$ by a path, i.e. a sequence of adjacent (colored) edges of the index graph. Therefore, proving two-connectedness of the index graph of a completely connected interaction graph is sufficient for establishing the minimal attractor space given by (8) because two-connectedness implies also one-connectedness.

Two-connectedness of the index graph of a completely connected interaction graph can be proved in three steps. In a first step, one proves two-connectedness for an oriented-star interaction graph (compare with figure A.1 (top)) with an arbitrary number of qubits. This can be achieved inductively. The first step of this inductive proof, which involves a two-qubit oriented-star interaction graph, is apparent. Continuing the induction, let us suppose that an N-qubit oriented-star interacting graph implies two-connectedness of the corresponding index graph. An $(N+1)$-qubit oriented-star interaction graph is formed by adding an $(N+1)$th qubit and $2(N+1)$ edges $e = 1(N+1)$ and $e' = (N+1)1$. As is apparent from the special case of $N = 2$ in figure A.1, the index graph resulting from the addition of one more qubit without connecting it yet to the rest of the interaction graph by edges has three dicomponents of continuity. One of these components is isomorphic to the index graph of an oriented-star interaction graph with N qubits whose vertexes have the $(N+1)$th qubit in the quantum state $|0\rangle$. The same applies to the second dicomponents of continuity apart from the fact that the $(N+1)$th qubit is in the quantum state $|1\rangle$. The index graphs of these two components can be transformed into each other by a bijective mapping of vertexes, edges and colors, i.e. they are color isomorphic. The third component is formed by the single vertex $(0, 0, \ldots, 0, 1)$. Hence, all three resulting dicomponents of continuity are two-connected. Let us now add also the $2(N+1)$ new colored edges $e = 1(N+1)$ and $e' = (N+1)1$. The colored edges with color $e = 1(N+1)$ connect the first and second dicomponent of continuity and the edges with color $e' = (N+1)1$ connect the second and the third one or they connect vertexes within the second one. The two-connectedness of the resulting index graph can be proved in a straightforward way by taking advantage of the color isomorphism between the first dicomponent of continuity and the second one. As an example, let us choose a vertex u_1 in the first dicomponent of continuity and a vertex v_1 in the second one. Due to the color isomorphism between both components, this pair of vertexes can be connected to an arbitrary other pair of vertexes by an appropriate sequence of adjacent colored edges applied to both vertexes, even if both final vertexes are located in the second component, for example. For this purpose, one connects vertex u_1 to a vertex that is adjacent to an edge with color $e = 1(N+1)$ in the first dicomponent of continuity and vertex v_1 to a vertex in the second component that is not adjacent to an edge $e = 1(N+1)$. Subsequently, the color $e = 1(N+1)$ connects these vertexes to vertexes in the second dicomponent of continuity. In view of the two-connectedness of this component, these vertexes can now be connected to any other pair of vertexes. Other cases can be proved in a similar way. Hence, the index graph induced by an oriented-star interaction graph is two-connected.

In the second step, it is proved that the index graph of an arbitrary interaction graph containing an oriented star is two-connected. Definitely, this is true because such an interaction graph induces in its index graph even more colored edges. Therefore, the two-connectedness of the index graph is not affected.

In the third step, one takes advantage of the fact that all strongly connected interaction graphs can be obtained from the complete interaction graph by successively removing edges.

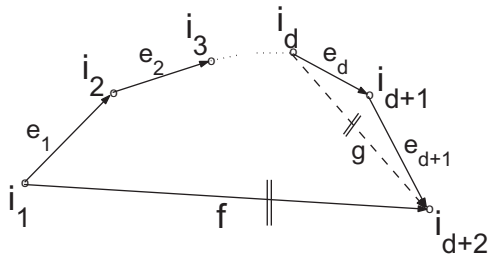

Figure A.2. Part of a strongly connected interaction graph. The edge f can be removed because it can be substituted by a path.

However, as strong two-connectedness of the index graph is a necessary condition for obtaining the minimal attractor space (8), one has to demonstrate that the two-connectedness of the index graph is not affected by such a removal of edges of the interaction graph as long as the interaction graph remains strongly connected. This property can be proved by induction with respect to the length d of a path connecting any pair of vertex pairs of the index graph. We start the inductive proof by considering a completely connected interaction graph and one of its paths of length $d = 2$ formed by the adjacent edges $e = ij$ and $f = jk$ of length unity and an edge $g = ik$ of length $d = 2$. In the corresponding index graph, the colored edge g has the same effect as applying the colored edges $fefe$. Thus, the colored edge g can be removed from the interaction graph without losing the two-connectedness of its induced index graph. Continuing the proof by induction, we consider a path of length $d + 1$ involving the adjacent edges $e_1 = i_1 i_2$, $e_2 = i_2 i_3, \ldots\ e_{d+1} = i_{d+1} d+2$ of an interaction graph under the assumption that all edges that can be substituted by paths of length d in this interaction graph can be eliminated without affecting the two-connectedness of the induced index graph (see figure A.2). If one inserts in this interaction graph an additional edge $g := i_d i_{d+2}$, one does not affect the two-connectedness of the induced index graph. By this insertion, qubits i_1 and i_{d+2} are connected by a path of length d, so that any direct edge between qubits i_1 and i_{d+2} can be removed without affecting the two-connectedness of the index graph. As a consequence, also any edge of an interaction graph that can be substituted by a path of length $d + 1$ can be removed without affecting the two-connectedness of the induced index graph. This completes the proof by induction. □

Let us finally comment on the fact that strong connectivity of the interaction graph is necessary for the attractor space of the form (8). If the interaction graph was not strongly connected, it would consist of at least of two dicomponents of continuity so that qubits in the first dicomponent are not coupled to qubits in the second component. For the induced index graph, this implies that binary indices that have vanishing indices for all qubits in the first component are not connected to binary indices that have non-vanishing indices for all qubits in the first component. Therefore, not all matrix elements in sets A_i of (A.3) are related and thus the set of attractors fulfilling (2) for $\lambda = 1$ is larger than the minimal set of base attractors. Therefore, for $\lambda = 1$, strongly connected interaction graphs constitute the largest set of interaction graphs with the attractor space given as (8).

A.1.2. The attractor space with $\lambda = -1$. We have already shown that strongly connected graphs of interaction imply that matrix elements of attractors with both indices in one of the sets A_i ($i \in \{1, 2, \ldots, 5\}$) of (A.3) are all equal. However, now the eigenvalue of the set of equations (A.2) is given by $\lambda = -1$. Strong connection implies that an arbitrary qubit is

the tail of some edge in the interaction graph. Thus, with both indices in the set A_1, an arbitrary edge yields the relation $X_{(\mathbf{0},\mathbf{0})} = -X_{(\mathbf{0},\mathbf{0})} = 0$. The same conclusion is obtained for matrix elements of $\hat{X}$ with indices in one of the sets A_2, A_3 or A_4 because of the relations $X_{(\boldsymbol{i},\mathbf{0})} = -X_{(\boldsymbol{i},\mathbf{0})} = X_{(\mathbf{0},\boldsymbol{i})} = -X_{(\mathbf{0},\boldsymbol{i})}$.

The case with indices in the set A_5 is more complicated. Depending on the number of qubits N, one has to distinguish two cases. If $N \geqslant 3$, one can always choose indices of the form $\boldsymbol{i} = (0, \boldsymbol{i}')$, $\boldsymbol{j} = (0, \boldsymbol{j}')$ with $\boldsymbol{i}' \neq \boldsymbol{j}'$. Applying an edge with the first qubit as the tail, i.e. as the control qubit, one obtains the relation $X_{(\boldsymbol{i},\boldsymbol{j})} = -X_{(\boldsymbol{i},\boldsymbol{j})} = 0$. Therefore, all matrix elements with indices from the set A_5 are zero. Hence, for $N \geqslant 3$, there is no non-zero attractor corresponding to eigenvalue $\lambda = -1$. Let us now consider the case of two qubits, i.e. $N = 2$. We cannot use the same argument again, because there is no such pair of indices. In this case, a successive application of edges of a strongly connected interaction graph yields the result

$$\begin{aligned} X_{((1,0),(0,1))} &= -X_{((1,1),(0,1))} = X_{((1,1),(1,0))} = -X_{((1,0),(1,1))} = X_{((0,1),(1,1))} \\ &= -X_{((0,1),(1,0))}. \end{aligned} \tag{A.4}$$

Finally, this confirms the validity of theorem 3.1 for $\phi = \pi/2$ and for the eigenvalue $\lambda = -1$.

A.2. The attractor space resulting from arbitrary conditional unitary couplings

For a general parameter $\phi \in (0, \pi)$ of the conditional unitary coupling (5), the equations for the attractors (2) can be rewritten in a form that is similar to (A.2). As an example, consider the resulting equations for two qubits a and b coupled by the conditional unitary transformation $\hat{U}_{ab}^{(\phi)}$. In order to simplify notation, let us skip all indices of the remaining $N-2$ qubits as they are not mixed by (2) for $\hat{U}_{ab}^{(\phi)}$. In this simplified notation, the resulting equations for the matrix elements of $\hat{X}$ are given by

$$\begin{aligned} &\lambda X_{0j}^{0i} = X_{0j}^{0i}, \\ &\lambda X_{10}^{0i} = X_{10}^{0i}\cos\phi + X_{11}^{0i}\sin\phi, \qquad \lambda X_{11}^{0i} = X_{10}^{0i}\sin\phi - X_{11}^{0i}\cos\phi, \\ &\lambda X_{0i}^{10} = X_{0i}^{10}\cos\phi + X_{0i}^{11}\sin\phi, \qquad \lambda X_{0i}^{11} = X_{0i}^{10}\sin\phi - X_{0i}^{11}\cos\phi, \\ &\lambda X_{10}^{10} = X_{10}^{10}\cos^2\phi + X_{11}^{10}\cos\phi\sin\phi + X_{10}^{11}\cos\phi\sin\phi + X_{11}^{11}\sin^2\phi, \\ &\lambda X_{11}^{11} = X_{11}^{11}\cos^2\phi - X_{11}^{10}\cos\phi\sin\phi - X_{10}^{11}\cos\phi\sin\phi + X_{10}^{10}\sin^2\phi, \\ &\lambda X_{11}^{10} = -X_{11}^{10}\cos^2\phi + X_{10}^{10}\cos\phi\sin\phi - X_{11}^{11}\cos\phi\sin\phi + X_{10}^{11}\sin^2\phi, \\ &\lambda X_{10}^{11} = -X_{10}^{11}\cos^2\phi + X_{10}^{10}\cos\phi\sin\phi - X_{11}^{11}\cos\phi\sin\phi + X_{11}^{10}\sin^2\phi \end{aligned} \tag{A.5}$$

with $i, j \in \{0, 1\}$.

Let us consider the eigenvalue $\lambda = 1$ first. In this case, these equations can be rewritten in the more concise form

$$X_{00}^{10}\sin(\phi/2) = X_{00}^{11}\cos(\phi/2), \tag{A.6}$$

$$X_{10}^{00}\sin(\phi/2) = X_{11}^{00}\cos(\phi/2), \tag{A.7}$$

$$X_{10}^{01}\sin(\phi/2) = X_{11}^{01}\cos(\phi/2), \tag{A.8}$$

$$X_{01}^{10}\sin(\phi/2) = X_{01}^{11}\cos(\phi/2), \tag{A.9}$$

$$2X_{11}^{10}\cos\phi = \left(X_{10}^{10} - X_{11}^{11}\right)\sin\phi, \tag{A.10}$$

$$X_{11}^{10} = X_{10}^{11}. \tag{A.11}$$

In the special case $\phi = \pi/2$, they reduce to the equations for the controlled-NOT coupling.

Each unitary action $\hat{U}_{ab}$ connects different matrix elements of a possible attractor $\hat{X}$. (A.6) connects matrix elements with indices from the set A_2. Similarly, (A.7) connects matrix elements with indices from the set A_3. Equations (A.8)–(A.10) connect matrix elements with indices from the set A_5. The major difference from the special case of controlled-NOT operations is the fact that (A.10) also connects matrix elements with indices from the set A_4 with those from the set A_5. However, this coupling does only involve differences of matrix elements with indices in A_4. From our proof for controlled-NOT operations, it follows that all matrix elements with indices in a given set A_i ($i \in \{1, \ldots, 5\}$) are connected if and only if the interaction graph is strongly connected. Therefore, we can conclude that also for $\phi \neq 0, \pi/2, \pi$ the base graphs are strongly connected graphs. For a base attractor $\hat{X}$, this implies that as soon as one of its matrix elements with indices from one of the sets A_i ($i \in \{1, \ldots, 5\}$) is defined, the other ones with indices in the same set are also determined. Hence, again the minimal attractor space corresponding to eigenvalue $\lambda = 1$ is 5D.

Let us now construct the set of minimal attractors. The attractor corresponding to the set of indices A_1 is apparently given by $\hat{X}_1 = |\mathbf{0}\rangle\langle\mathbf{0}|$. For the determination of the attractor $\tilde{\hat{X}}_2$ that corresponds to the set A_2, we start from the arbitrarily chosen matrix element $(\tilde{\hat{X}}_2)_{\mathbf{0}}^{\mathbf{1}} = (\sin(\phi/2))^{N-1}$ with $\mathbf{1} = (1, 1, \ldots, 1)$ and $\mathbf{0} = (0, 0, \ldots, 0)$. (A.6) implies $(\tilde{\hat{X}}_2)_{\mathbf{0}}^{\boldsymbol{i}} = (\sin(\phi/2))^{\tau(\boldsymbol{i})-1}(\cos(\phi/2))^{N-\tau(\boldsymbol{i})}$ with $\mathbf{0} \neq \boldsymbol{i} \in \mathrm{I}_N$. All other elements of this attractor are equal to zero. In a similar way, we can determine the matrix elements of the attractor $\tilde{\hat{X}}_3$ that corresponds to the set A_3. It is given by $(\tilde{\hat{X}}_3)_{\boldsymbol{i}}^{\mathbf{0}} = (\sin(\phi/2))^{\tau(\boldsymbol{i})-1}(\cos(\phi/2))^{N-\tau(\boldsymbol{i})}$ with all other matrix elements vanishing. Consider now the indices from the set A_4. The corresponding matrix elements are determined by (A.10) and are therefore connected to matrix elements with indices from the set A_5. If the matrix elements of an attractor corresponding to the set of indices A_5 are given, according to (A.10), only a single matrix element with indices from the set A_4 can be chosen arbitrarily. Setting all matrix elements with indices not contained in the set A_4 to zero, this free choice of this single matrix element yields the attractor $\tilde{\hat{X}}_5 = I - |\mathbf{0}\rangle\langle\mathbf{0}|$. The last attractor $\tilde{\hat{X}}_4$ corresponding to the index set A_5 can be constructed in a similar way as the attractors $\hat{X}_2$ and $\hat{X}_3$. It is given by $(\tilde{\hat{X}}_4)_{\boldsymbol{j}}^{\boldsymbol{i}} = (\sin(\phi/2))^{\tau(\boldsymbol{i})+\tau(\boldsymbol{j})-2}(\cos(\phi/2))^{N-\tau(\boldsymbol{i})-\tau(\boldsymbol{j})}$ with $\boldsymbol{i}, \boldsymbol{j} \neq \mathbf{0}$. By orthonormalization of these attractors, we finally arrive at the set of orthonormal attractors (8).

For the eigenvalue $\lambda = -1$, the set of equations (A.5) can be rewritten in the concise form

$$\begin{aligned} X_{0j}^{0i} &= -X_{0j}^{0i}, \quad & X_{10}^{0i}\cos(\phi/2) &= -X_{11}^{0i}\sin(\phi/2), \\ X_{10}^{10} &= -X_{11}^{11}, \quad & X_{0i}^{10}\cos(\phi/2) &= -X_{0i}^{11}\sin(\phi/2), \end{aligned} \tag{A.12}$$

with $i, j \in \{0, 1\}$. Therefore, the determination of the structure of minimal attractors is analogous to the case of the controlled-NOT interaction, i.e. $\phi = \pi/2$. Thus, one can show that for $N \geqslant 3$ there is no non-zero attractor for strongly connected graphs, and for $N = 2$ there

is only one solution, namely

$$\begin{aligned}&\sin(\phi/2)X_{((1,0),(0,1))} = -\cos(\phi/2)X_{((1,1),(0,1))}\\&= \cos(\phi/2)X_{((1,1),(1,0))} = -\cos(\phi/2)X_{((1,0),(1,1))}\\&= \cos(\phi/2)X_{((0,1),(1,1))} = -\sin(\phi/2)X_{((0,1),(1,0))}.\end{aligned} \tag{A.13}$$

This completes the proof of theorem 3.1. □

References

[1] Feynman R P 1982 *Int. J. Theor. Phys.* **21** 467
[2] Weimer H, Müller M, Lesanovsky I, Zoller P and Büchler H P 2010 *Nat. Phys.* **6** 382
[3] Gordon G, Bhaktavatsala Rao D D and Kurizki G 2010 *New J. Phys.* **12** 053033
[4] Albert R and Barabasi A-L 2002 *Rev. Mod. Phys.* **74** 47
[5] Duan L-M and Monroe C 2010 *Rev. Mod. Phys.* **82** 1209
[6] Choi K S, Deng H, Laurat J and Kimble H J 2008 *Nature* **452** 67
[7] Nielsen M A and Chuang A L 2000 *Quantum Computation and Quantum Information* (Cambridge: Cambridge University Press)
[8] Joos E, Zeh H D and Kiefer C 2002 *Decoherence and the Appearance of a Classical World in Quantum Theory* (Heidelberg: Springer)
[9] Zurek W 2003 *Rev. Mod. Phys.* **75** 75
[10] Caruso F, Chin A W, Datta A, Huelga S F and Plenio M B 2010 *Phys. Rev.* A **81** 062346
[11] Caruso F, Huelga S F and Plenio M B 2010 *Phys. Rev. Lett.* **105** 190501
[12] Lengwenus A, Kruse J, Schlosser M, Tichelmann S and Birkl G 2010 *Phys. Rev. Lett.* **105** 170502
[13] Scarani V, Ziman M, Štelmachovič P, Gisin N and Bužek V 2002 *Phys. Rev. Lett.* **88** 097905
[14] Ziman M and Bužek V 2005 *Phys. Rev.* A **72** 022110
[15] Koniorczyk M, Varga A, Rapcan P and Bužek V 2008 *Phys. Rev.* A **77** 052106
[16] Benenti G and Palma G M 2007 *Phys. Rev.* A **75** 052110
[17] Gennaro G, Benenti G and Palma G M 2009 *Phys. Rev.* A **79** 022105
[18] Pineda C and Seligman T H 2007 *Phys. Rev.* A **75** 012106
[19] Novotný J, Alber G and Jex I 2009 *J. Phys. A: Math. Theor.* **42** 282003
[20] Novotný J, Alber G and Jex I 2010 *Cent. Eur. J. Phys.* **8** 1001
[21] Bengtsson I and Życzkowski K 2006 *Geometry of Quantum States* (Cambridge: Cambridge University Press)
[22] Bhatia R 2007 *Positive Definite Matrices* (Princeton, NJ: Princeton University Press)
[23] Diestel R 2010 *Graph Theory* (Heidelberg: Springer)
[24] Schulman L S and Gaveau B 2006 *Phys. Rev. Lett.* **97** 240405